Contents list available at CBIORE journal website

International Journal of Renewable Energy Development

Journal homepage: https://ijred.cbiore.id

Research Article

Optimal hydropower potential assessment in semi-arid regions

Imane El Kasimi*, Moulay Driss Hasnaoui, Driss Khomsi, Ahmed Bouziane, Amal Aboulhassane

Hydraulic System Analysis Team (HSAT) Laboratory, Mohammadia School of Engineering, Mohammed V University, Rabat, Morocco

Abstract. While hydropower is a cornerstone of global renewable energy strategies, its development in semi-arid regions remains insufficiently explored. Limited and highly variable water availability often discourages comprehensive assessments of its potential. In particular, run-of-river hydropower, despite its environmental and economic advantages, remains largely underexplored in these contexts due to its sensitivity to flow variability. This study evaluates the theoretical hydropower potential of run-of-river schemes within the semi-arid Grou watershed, a major tributary of the Bouregreg river in Morocco, with a focus on optimizing energy production under dry hydrological conditions. Hydrological modeling was applied using the Soil and Water Assessment Tool (SWAT), enabling the generation of flow-duration curves across the river network. These curves were then used to develop energy-duration curves, allowing for the identification of multiple optimal design flows. Consequently, instead of relying on a single turbine, the study explores the deployment of modular turbines per plant, each tailored to specific flow regimes, thereby expanding the range of exploitable run-of-river hydropower. Results indicate an untapped hydropower potential of approximately 32.4 MW per meter of head, with outputs of 31.5 MW, 783.3 kW, and 98.9 kW for high, moderate, and low flows, respectively. These findings highlight the feasibility of run-of-river hydropower in semi-arid regions and underscore the importance of adaptive turbine systems in enhancing sustainable energy production, specifically in water-scarce environments such as Morocco.

Keywords: Run-of-river, Hydrological modeling, SWAT, Flow-duration curve, Modular turbines.

Received: 10th Nov 2024; Revised: 5th May 2025; Accepted: 25th June 2025; Available online: 15th July 2025

1. Introduction

Adopting renewable energy is crucial in combating greenhouse gas emissions; therefore, it is considered an essential pillar in the mitigation strategies defined by the United Nations Framework Convention on Climate Change. While all renewable energy sources contribute to reducing fossil fuel dependence, hydropower is particularly reliable and can be adjusted to meet demand throughout the day and across seasons (Killingtveit, 2020). Conversely, other sources are mostly intermittent and may fail during periods of extreme need (IRENA, 2023a). From a technical standpoint, hydropower technology is mature, as it is one of the oldest and most efficient energy sources (Killingtveit, 2020). This underscores its role as the most prominent renewable energy globally, contributing to nearly 53% of renewable electricity production and approximately 15% to the total electricity production in 2022 (IRENA, 2024). It is also considered one of the most economically efficient sources of electricity, with a lower levelized cost of electricity compared to fossil-fueled energies during the 2010-2021 period (IRENA, 2023b). In Morocco's case hydropower is the leading renewable energy source, (Védie, 2020). By 2015, during COP21, the country raised its ambition to increase the share of hydropower in the national energy mix by 12%, to be achieved through the development of 1,330 MW of additional capacity by 2030 (El Hafdaoui, Khallaayoun, & Al-Majeed, 2025).

Given the significance of hydropower, the question arises as to whether the potential of watersheds has been fully exploited. In fact, the International Energy Agency highlights that nearly 50% of the economic hydropower potential remains untapped, with a significant portion located in Africa (IEA, 2021; IRENA, 2023b). Hence, substantial opportunities for hydropower production have yet to be efficiently harnessed to meet the objectives of the climate change policies (IRENA, 2023b).

In this context, run-of-river (RoR) hydropower plants have emerged as a key contributor to the renewable energy mix, particularly in supporting rural electrification in developing countries (Malhan & Mittal, 2021). The RoR scheme typically includes a small intake weir constructed in a section of the river, creating a small impoundment. Water is then directed toward a forebay, which regulates elevation for stable power generation. A channel called the penstock then guides the water under pressure to the powerhouse, where a turbine transforms the hydraulic energy of the flow into electricity. Finally, the water is discharged at the plant's outlet. Power is generated using the water flow and the hydraulic head H, which is defined as the difference in altitude between the surface of the water level behind the weir and the placement of the turbine. Typically, RoR systems exploit heads ranging from a few meters to over 15 m and can produce up to 10 MW (Skoulikaris, 2021).

Recently, there has been a growing interest in these hydropower systems largely due to their numerous socioeconomic advantages (Nedaei & Walsh, 2022). They

* Corresponding author
Email: elkasimi@emi.ac.ma (I. El Kasimi); Telephone: +212645392922

https://doi.org/10.61435/ijred.2025.60831
ISSN: 2252-4940/© 2025.The Author(s). Published by CBIORE

require less construction time and costs than plants with similar capacity (Ibrahim *et al*., 2019). RoR hydropower systems are generally associated with low ecological impacts due to their minimal interference with the natural flow regime. With proper design and environmental safeguards, they offer a more sustainable energy option with minimal harm to aquatic ecosystems and maintain sediment, thermal and chemical conditions (Kuriqi *et al*., 2021). In addition to their environmental advantages, RoR plants are considered one of the most affordable renewable energy options, a factor that attracts investments, especially in developing countries (IRENA, 2023a). As a result, there has been an increasing number of studies evaluating their potential, reflecting the growing recognition of their role in sustainable energy production (Kuriqi *et al*., 2021).

In dry climates and water-scarce regions, RoR plants offer more adaptable hydropower solutions. As shown in the case of the Tsiknias river in Greece, low design discharge values allow such systems to remain functional and productive despite prolonged dry periods and fluctuating streamflow conditions (Tzoraki, 2020). Moreover, they have demonstrated notable resilience under climate change conditions, maintaining up to 75–80% of their generation potential despite projected runoff declines (Skoulikaris, 2021).

A typical approach to assessing RoR hydropower potential begins with a comprehensive watershed analysis, which can be complemented by economic, environmental, and social impact assessments (ESMAP, 2021). Therefore, an accurate hydropower potential evaluation begins with the proper watershed characterization. In this sense, geographic information systems (GIS) and remote sensing (RS) are suitable tools largely used by researchers. Bhattarai *et al.* (2024) used GIS software and RS maps to evaluate the topographic characteristics, land use, and land cover of a basin in Nepal for hydropower production. In addition to these functionalities, Wangchuk *et al*. (2024) emphasized that integrating GIS within Building Information Modeling (BIM) enhances hydropower project planning, particularly by supporting early-stage feasibility assessments. In the study by Golgojan *et al.* (2025) employed a GIS and RS techniques to estimate the hydrological, technical, financial, and realizable RoR hydropower potentials across Great Britain. Furthermore, Hedger *et al*. (2025) used GIS and RS tools to evaluate land use impacts and ecological risks from RoR plants in Norway by analyzing satellite imagery and elevation data to assess construction footprints and their overlap with sensitive habitats and species.

In general, GIS tools are combined with hydrological models to assess the potential of hydropower plants effectively. One of the most widely employed models in this domain is the Soil and Water Assessment Tool (SWAT). For example, Dilnesa (2022) used the SWAT model to locate 20 potential hydropower generation sites in Ethiopia's Temcha watershed. The flexibility

Table 1
Summary of the literature review

Reference	Study objective	Tools used	Key findings
Bhattarai *et al.* (2024)	Assess gross, technical, and economic hydropower potential in the Sunkoshi River Basin in Nepal, using integrated GIS and SWAT modeling.	GIS, SWAT model	Optimal sites for RoR were selected based on hydropower potential, environmental considerations, and economic feasibility. This approach is expected to reduce time for site identification and cost of extensive fieldwork.
Dilnesa (2022)	Evaluate the hydropower potential of RoR plants in Ethipio's Temcha watershed.	GIS, RS, SWAT model	Significant energy production potential was identified, particularly in the upper course of the river, highlighting the importance of using GIS-based hydrological assessments to support effective site selection.
Garcia *et al.* (2024)	Evaluate the impacts of environmental flow requirements and climate change on RoR hydropower in the Catalan River Basin District.	SWAT+, S+ HydPower	The S+ HydPower tool proved effective in assessing RoR viability and informing sustainable energy planning. It also demonstrated that hydropower in the Catalan River is more vulnerable to climate change than to environmental flow implementation.
Golgojan *et al.* (2025)	Provide a UK-wide assessment of RoR hydropower potential including financial, technical, and environmental constraints.	GIS, G2G hydrological model	A comprehensive framework was developed to assess RoR hydropower in Great Britain. The approach integrates hydrological, technical, financial, and environmental factors to guide sustainable development.
Hedger *et al.* (2025)	Evaluate the environmental impacts small-scale hydropower plants in Norway.	Remote sensing, GIS	The small hydropower plants have an overall low environmental impact on terrestrial biota and instream fish in Norway due to their small footprint, and they contribute to local and regional energy production
Pranoto *et al.* (2024)	Assess sustainability of RoR plants in Indonesia's Citarum watershed considering future land use and sedimentation.	CA-Markov model, IDRISI TerrSet model, SWAT model	An innovative modeling approach was established to assess water yield, erosion, and sedimentation, emphasizing the need to factor these into sustainable hydropower planning
Shrestha *et al.* (2020)	Evaluate hydrological alterations caused by climate change and reservoir operations.	GIS, Remote Sensing, SWAT, HydRoR	Climate change was found to affect seasonal flow patterns and extreme water conditions in hydropower reservoirs. In addition, optimizing reservoir rule curves was identified as essential for balancing power generation with ecological requirements.
Wangchuk *et al.* (2024)	Review the adoption of BIM at all stages of hydropower infrastructure development and assess its potential.	Systematic literature review using PRISMA framework	Integrating BIM enhances collaboration, design efficiency, and sustainability in hydropower projects. Although adoption remains limited to early project phases and specific regions, lifecycle-wide BIM implementation should improve project resilience and management.

of the SWAT model facilitated its combination with a tool called HydRoR, which determines the energy generated by a plant using predefined operational conditions of the dam (Shrestha *et al.*, 2020). Building on such integrated approaches, Garcia *et al.* (2024) combined the SWAT model with the custom-built S+HydPower tool within a GIS environment to simulate the combined effects of climate change and environmental flow policies on RoR hydropower systems. Similarily, Pranoto *et al.* (2024) applied the SWAT model to simulate future water supply, erosion rates, and sedimentation risks under projected land use scenarios in the Citarum watershed in Indonisia. In summary, Table 1 provides a structured overview of the cited studies, summarizing their objectives, tools, and main findings. It underscores the importance of GIS software, RS techniques, and hydrological modeling in advancing hydropower assessment. While some studies have focused on identifying new potential sites for RoR hydropower plants, others have evaluated the performance and sustainability of existing installations. Additionally, several approaches integrate hydrologic, topographic, economic, environmental, and climate change considerations to enhance hydropower potential and support its long-term viability.

Despite their multiple advantages, the main challenge of RoR plants is the absence of a reservoir. Therefore, power generation depends on streamflow variations, which leads to the vulnerability of the plant's output to uncertainties in hydrological conditions (Thakur *et al.*, 2024). As a result, an adequate potential assessment requires an optimal estimation of both parameters: the flow discharge and the head (Tsuanyo *et al.*, 2023). While the head is largely dictated by the watershed's topography, the available flow varies throughout the year. One key challenge is selecting the appropriate design discharge that determines the plant's energy output. In some cases, the design flow chosen corresponds to the flow available for at least 250 days per year to ensure reliability even during dry periods (Tsuany *et al.*, 2023). However, other approaches consider lower flow thresholds, available 180 days or 100 days per year (Moshe & Tegegne, 2022; Dhaubanjar *et al.*, 2024). This variability underscores the absence of a clear-cut choice when it comes to selecting the design flow of the RoR power plant.

In addition, the deployment of RoR schemes remains largely limited in dry regions. In fact, the World Small Hydropower Development Report highlights that only 4% of the estimated RoR potential has been developed in Northern Africa, a region characterized predominantly by a semi-arid climate (UNIDO & ICSHP, 2022). This underscores both the significance of the available resources and the limited interest in developing hydropower in such environments. In Morocco's case, the same report identifies untapped potential, supporting data, and an existing legislative framework for the deployment of RoR plants. Nevertheless, these hydropower schemes, which are central to this study, are not currently incorporated into the country's national energy strategy. This is primarily due to a lack of public interest and limited research focus on the subject (UNIDO & ICSHP, 2022). Moreover, in these climatic conditions, careful consideration must be given to the technical design parameters, especially the selection of the optimal design flow (Tzoraki, 2020).

Thus, the primary aim of our research is to develop a framework for an assessment of the optimal RoR hydropower potential within any watershed, even under dry conditions. In our case study, we have chosen the Grou watershed in Morocco, specifically because hydropower has never been produced in this region. Our approach focuses on developing the flow-duration curves (FDC). These graphs can be derived following hydrological modeling, which was performed by the SWAT model. Finally, to fully exploit the potential of the Grou watershed, we proposed placing modular turbines at each RoR plant, enabling hydropower generation across different discharge ranges. Specifically, we considered three levels of production: high, moderate, and small-scale.

2. Materials and methods

The theoretical hydropower is defined as the power generated by a power plant under ideal conditions, assuming the absence of turbine inefficiency and head losses throughout the entire system. Consequently, it mainly depends on two important parameters: discharge and the head. It can be estimated using the following formula (Killingtveit, 2020):

$$\boldsymbol{P = \gamma * Q * H} \quad (1)$$

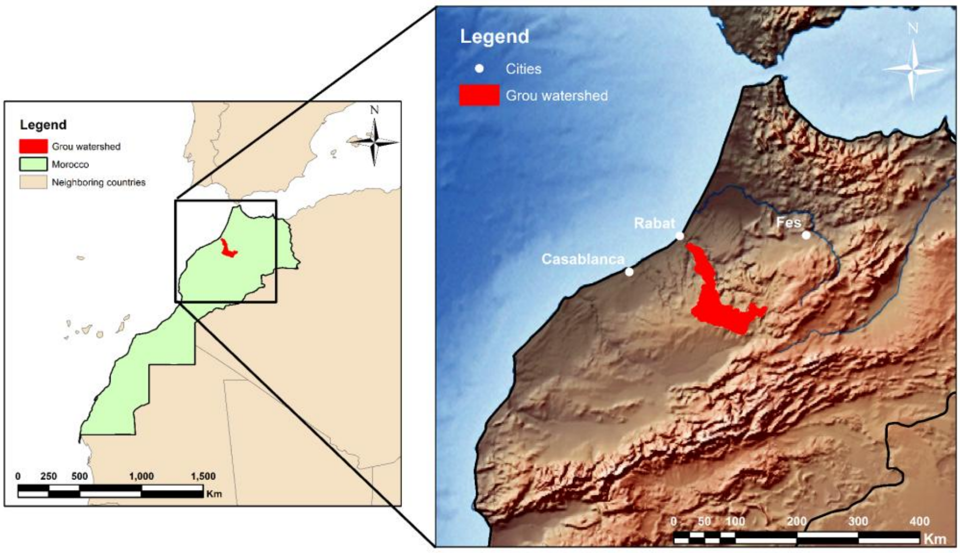

Fig. 1 Location of the Grou watershed in Morocco (ESRI, 2013, Natural Earth, 2009)

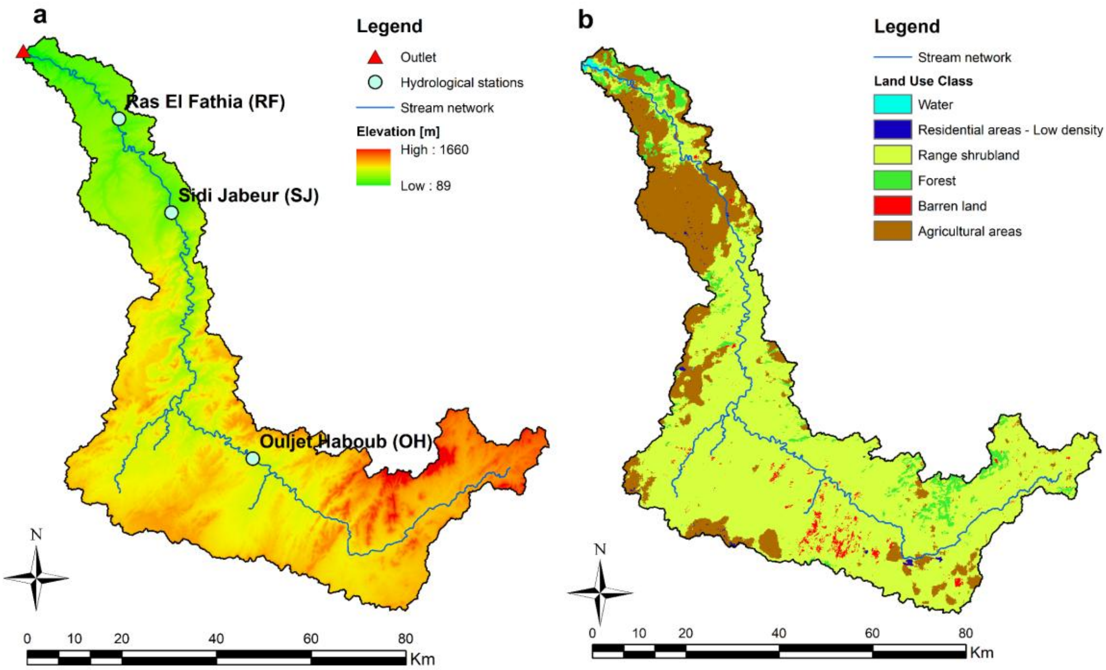

Fig. 2 DEM (a) and LULC map (b) of the Grou watershed (JAXA, 2014, Karra *et al*., 2021)

Where: P is the power generated by the plant [W], γ is the specific water weight [N/m^3], Q is the discharge [m^3/s] and H is the head [m].
The steps of the framework developed for this study are summarized as follows:

- Select potential locations for RoR plants along the watershed's streams.
- Execute the SWAT model to assess the streamflow discharges at each potential site.
- Plot the flow-duration curve (FDC) at each location.
- Generate the energy-duration curve (EDC) to determine the optimal theoretical hydropower potential at each location

2.1 Study area

The study area is the Grou watershed, the second major tributary of the Bourgreg river in Morocco. Its outlet is located at the coordinates (33.892641, -6.754918), situated 6 km upstream of the Sidi Mohamed Ben Abdellah Dam, which has a major role in supplying drinking water to the Atlantic coastal region, from the Salé-Rabat area to Casablanca (Fig. 1). The Grou watershed covers an area of 3 755 km² with elevations ranging from 89 m to 1 660 m above sea level, as seen in the Digital Elevation Map (DEM) in Fig. 2a. It receives an average annual rainfall of 323 mm, and the temperature varies between a maximum of 24 °C and a minimum of 11 °C (1977-2020). The watershed's climate can be classified as a semi-arid Mediterranean climate with a noticeable influence of the ocean, which is approximately 23.5 km downstream of its outlet (Cherrad, 1997). The majority of the watershed is covered by shrubland and agricultural areas which account for 74% and 20.5%, respectively, as shown in the Land Use/Land Cover map (LULC) in Fig. 2b.

2.2 Potential RoR locations

The evaluation of hydropower potential heavily depends on the methodological approach employed, with the initial step typically being the selection of plant sites. The most common way for this is to place plants at equal distances along the streams (Alcalá *et al*., 2021). This spacing criterion must take into consideration multiple variables. Notably, the distance between the diversion and the power plant outlet should be minimized to help restore the river's natural flow and cut the installation costs by shortening the penstock (Bejarano *et al*., 2019; Amougou *et al*., 2022). Moreover, it is essential to ensure adequate spacing between consecutive sites to prevent the tailrace of one site from affecting the pondage of the next (Moshe & Tegegne, 2022). In our approach, a 5 km distance between two successive plants was considered, which not only

Table 2
Input data and sources for the SWAT model

Data	Description	Source
DEM	12.5 m resolution	ALOS PALSAR (JAXA, 2014)
Land use / Land cover	10 m resolution, 2020 map	Sentinel-2 10m Land Use/Land Cover (Karra *et al*., 2021)
Soil Map	50 km resolution	The Food and Agriculture Organization of the United Nations (FAO, 1971-1981)
Rainfall and streamflow discharge	Daily data, period: 1977-2020	The Moroccan Ministry of Equipment and Water
Temperature, solar radiation, wind speed, and relative humidity	Daily data, period: 1977-2020	ERA-5 Land (Muñoz Sabater, 2019)

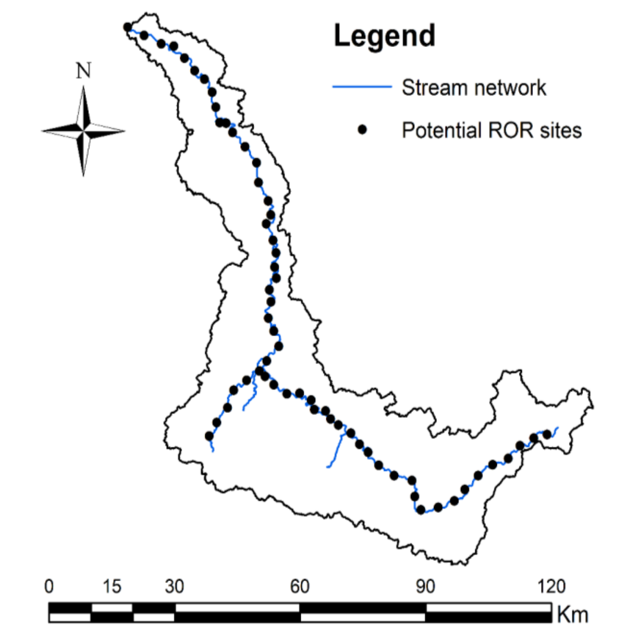

Fig. 3 Locations of potential RoR plants

offers the flexibility to reduce the length between the diversion and the outlet but also provides a sufficient gap between consecutive hydropower sites for environmental reasons. For this purpose, the DEM was employed to generate the watershed's stream network, as shown in Fig. 2. Starting at the outlet, the streams were divided using the 5 km distance, where the point separating two segments represents the diversion of each power plant. In this study, 60 potential plant sites were identified through this discretization process, as illustrated in Fig. 3.

In this study, the hydropower potential of the Grou watershed will be evaluated for a hypothetical head of 1 m. However, the elevation difference between two consecutive sites ranged from 5 m to 42 m. These values enable generating hydropower by utilizing the natural topographical drop or by constructing small weirs, which can theoretically create hydraulic heads of at least 5 m. Therefore, the real potential exceeds the estimates from our study, as reflected by equation (1); the power generated at each site is multiplied by the value of the existing head.

2.3 Hydrological modeling

The second step of our approach is dedicated to hydrological modeling, aiming to simulate river discharge using meteorological and spatial data in close agreement with measured flows.

2.3.1 SWAT model

In order to assess the streamflow Q needed for equation (1), the semi-distributed continuous model SWAT was used (Arnold *et al.*, 1998; SWAT, 2012). More than 6800 papers in peer-reviewed journals have cited the use of SWAT at different scales of gauged and ungauged basins (CARD & ISU, 2023). Its implementation covered major points such as: (i) surface runoff simulation for water sources, floods, and pollution management in watersheds; (ii) the spatial and temporal distribution of non-point pollution originating from urban, mining zones, and agricultural activities; (iii) land use and climate change impact on the hydrological cycle, soil erosion, sediment deposition, and pollution (Janjić and Tadić, 2023). Using topography data, the SWAT model divides the watershed into multiple sub basins, which are further subdivided into Hydrologic Response Units (HRUs) with unique land use, management, slope, and soil characteristics. The SWAT model then employs the water balance equation and simulates for hydrological components such as surface runoff, evapotranspiration, percolation at daily, monthly, and annual time steps (Tan *et al.*, 2020).

A set of spatial data is required to build a SWAT model, including a DEM, a LULC map, and a soil map. These maps help create the stream networks and delineate the sub basins and HRUs. Several daily hydrometeorological input data are also needed, such as rainfall, maximum and minimum air temperature, solar radiation, wind speed, and relative humidity. All the input data employed in our SWAT model are detailed in Table 2. In particular, the relative humidity was calculated using the Magnus formula, based on the dew temperature data retrieved from the ERA5-Land dataset (Alduchov and Eskridge, 1996). The daily precipitation data were collected from the Moroccan Ministry of Equipment and Water at three hydrometric stations, as shown in Fig. 2: Ras El Fathia (RF) (33.10773345, -6.25367387), Sidi Jabeur (SJ) (33.57816988, -6.42637079), and Ouljet Haboub (OH) (33.10773345, -6.25367387).

2.3.2 Calibration and validation of the SWAT model

The initial run of the SWAT model is performed using default parameters. Therefore, calibration and validation are a crucial subsequent step to adjust these parameters while minimizing the difference between the observed and simulated results. For this purpose, the daily discharge data measured at the hydrological stations from 1977 to 2009 were used for model calibration. The final set of calibrated parameters must be validated using different hydrological and weather data; therefore, data from 2010 to 2020 were employed for validation. The provided data set was divided while ensuring the inclusion of wet, moderate, and dry years in both the calibration and validation steps (Arnold *et al.*, 2012). In particular, the average and standard deviation of daily discharge values were approximately equal between the calibration and validation periods, ensuring comparable hydrological variability.

The evaluation of the SWAT model is executed by using the semi-automated SUFI2 program of the SWAT-CUP software (SWAT-CUP, 2007). The calibration program is executed by optimizing an objective function. Amongst the most widely used functions in runoff modeling are the Nash-Sutcliffe coefficient (NSE) and the Percent Bias (PBIAS) defined by Nash & Sutcliffe (1970) and Moriasi *et al.* (2007), respectively as follows:

$$\boldsymbol{NSE = 1 - \frac{\sum_{i=1}^{n}(O_i - P_i)^2}{\sum_{i=1}^{n}(O_i - \bar{O})^2}} \quad (2)$$

$$\boldsymbol{PBIAS = \frac{\sum_{i=1}^{n}(O_i - P_i)}{\sum_{i=1}^{n} O_i} * 100} \quad (3)$$

Where: O_i is the measured discharge [m^3/s], P_i is the simulated discharge [m^3/s], $\bar{O}$ is the mean of measured discharges [m3/s] and n is the total number of measured discharges.

The NSE coefficient compares the simulated data's residual variance to the observed data's initial variance, and it ranges from -∞ to 1, with an optimal value of 1 (Nash & Sutcliffe, 1970). The PBIAS evaluates the deviation of the simulated data from

Table 3
SWAT performance metrics for daily runoff (Kalin *et al*., 2010)

Performance	NSE	PBIAS
Very Good	$\mathrm{NSE} \geq 0.7$	$\lvert\mathrm{PBIAS}\rvert \leq 0.25$
Good	$0.5 \leq \mathrm{NSE} < 0.7$	$0.25 < \lvert\mathrm{PBIAS}\rvert \leq 0.5$
Satisfactory	$0.3 \leq \mathrm{NSE} < 0.5$	$0.5 < \lvert\mathrm{PBIAS}\rvert \leq 0.7$
Unsatisfactory	$\mathrm{NSE} < 0.3$	$\lvert\mathrm{PBIAS}\rvert > 0.7$

the observed data with an optimal value of 0. A positive PBIAS indicates the tendency of the model to overestimate the discharge, whereas a negative value indicates a tendency of underestimation (Moriasi *et al*., 2007). In this study, the interpretation provided by Kalin *et al*. (2010) for the model's performance for daily streamflow simulations was used and is detailed in Table 3.

The calibration and validation procedures followed the methodology described by Arnold *et al*. (2012), using the NSE coefficient as the objective function. As recommended by Yu, Noh, and Cho (2020), the initial calibration round was conducted with 1000 simulations to significantly enhance model performance, followed by two additional rounds of 500 simulations each. The detailed steps of the procedure are as follows:

- The most sensitive parameters related to surface runoff were selected based on their frequent use in runoff calibration studies.
- An initial uncertainty range of ±20% to ±30% around each parameter's default value was assigned.
- The SUFI-2 algorithm was used to perform the calibration.
- Model performance was assessed by analyzing simulated versus observed hydrographs, along with statistical indicators such as the p-factor, r-factor, NSE, and PBIAS.
- Parameters with high p-values, indicating low sensitivity, were excluded from further calibration rounds.
- The following calibration rounds involved refining parameter ranges based on model response, with particular attention given to spatial calibration at the sub-basin level when necessary.
- Calibration was repeated until acceptable NSE and PBIAS values, a high p-factor, and a low r-factor were obtained.
- The final set of calibrated parameters was used for validation over an independent time period.

2.4 Flow-duration curve

The flow-duration curve (FDC) is a graphical representation of the frequency or number of days at which flow is equaled or exceeded. The use of FDCs is well-established in hydropower assessment studies (Moshe & Tegegne, 2022; Kamran, 2022), as well as for various other purposes (Leong & Yokoo, 2021).

In order to construct the FDCs, Vogel and Fennessey (1994) recommend using non-parametric quantile estimation procedures, particularly L-estimators, which are defined as linear combinations of the order statistics. These estimators have been proven to be more efficient than single order statistics and can produce smoother estimates of the FDCs (Vogel & Fennessey, 1994). Therefore, the Harrell-Davis (HD) estimator was used in this study (Harrell and Davis, 1982). The mathematical definition of the HD estimator is presented in Table 4.

To accurately assess the annual hydropower production within a watershed, the FDC must capture typical annual flow conditions. However, constructing an FDC based on the period of record reflects the long-term streamflow behavior rather than the yearly flow variations (Searcy, 1959; Sarigil, *et al*., 2024). Therefore, Vogel and Fennessey (1994) suggested employing the median annual flow-duration curve (AFDC) instead, as it represents an average year that is less skewed by unusual weather conditions.

Thus, a median year must be identified from the period of recorded data. For this purpose, the closest station to the outlet, the RF station, was chosen as the hydrological representative of the watershed. By calculating the annual runoff for each year within the observation period, it was determined that 1998 was the median year, although it was slightly drier according to measurements from other stations. Thus, using the streamflow output from the SWAT model and the HD estimator, the 1998 AFDC was constructed at each potential hydropower plant site. Furthermore, the model's performance will be evaluated by comparing the simulated and measured annual FDCs for each year of the observation period using the NSE, as described by Blum, Archfield, and Vogel (2017).

2.5 Evaluation of the optimal theoretical hydropower

To determine the optimal theoretical power production at a site, the following procedure was adopted:

- Construct the power-duration curve (PDC): Using the median AFDC, the theoretical power corresponding to each discharge value is calculated using equation (1) and plotted against the number of days in a year.
- Plot the energy-duration curve (EDC): The theoretical power from the PDC is multiplied by the number of hours

Table 4
Definition of the HD estimate and its weight function (Harrell and Davis, 1982).

Function	Definition	Description
HD estimator	$Q_{p,HD} = \sum_{i=1}^{n} W_i q_i$	For n observations of streamflow q_i ($1 \leq i \leq n$) arranged in ascending order, $Q_{p,HD}$ is the HD estimate of the pth quantile with a probability of exceedance p ($0<p\leq1$). The estimate assigns a weight W_i to each observation q_i.
Weights of the HD estimator	$W_i = I_{i/n}[p(n+1),(1-p)(n+1)] - I_{\frac{i-1}{n}}[p(n+1),(1-p)(n+1)]$	The weights of the HD estimate $Q_{p,HD}$ are derived from the beta distribution. $I_x[a,b]$ represents the incomplete beta function, where n is the sample size and p is the exceedance probability.

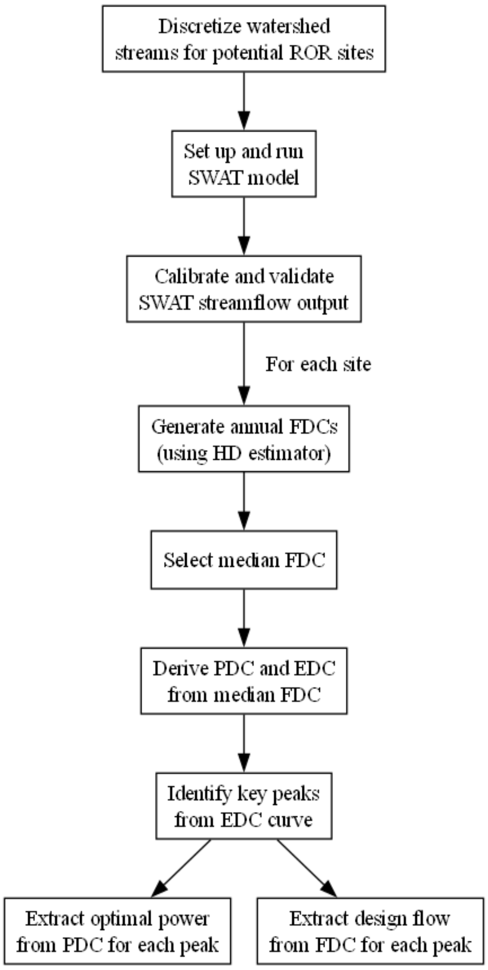

Fig. 4 Flowchart for assessment of optimal RoR potential within semi-arid watersheds.

of its availability during the year, as formulated by Killingtveit (2020):

$$\boldsymbol{E = P.d.24} \quad (4)$$

Where: E is the annual energy output [Wh], P is the power generated [W] and d is the number of days of availability of the power P from the PDC.

- Identify local maxima on the EDC: These peaks represent multiple optimal production scenarios, indicating the various power levels that maximize annual energy output.
- Determine the corresponding power potential: Each peak of the EDC reflects a theoretical hydropower production scenario that could be considered optimal for the site.

Given the presence of multiple optimal scenarios per site, a combination of modular turbines is proposed to efficiently capture the full range of hydropower potential. The design flow for each turbine can be determined by identifying the discharge value corresponding to each peak in the EDC. Accordingly, Fig. 4 illustrates the methodological framework developed and implemented in this study.

3. Results and Discussion

After developing the SWAT model, its accuracy is evaluated using the NSE and PBIAS statistics. These assessments will ensure the reliability of the simulated streamflow before generating the AFDCs and their corresponding EDCs for each of the 60 selected RoR sites. The shape and variability of the EDCs across the watershed will then serve to identify multiple optimal design flows per site.

3.1 Calibration and validation of the SWAT model

The calibration process for the SWAT model resulted in identifying the most sensitive parameters and their best calibrated values, as presented in Table 5. The high sensitivity of soil-related parameters (SOL_BD, ESCO, and CN2) suggests that soil properties, evaporation processes, and runoff

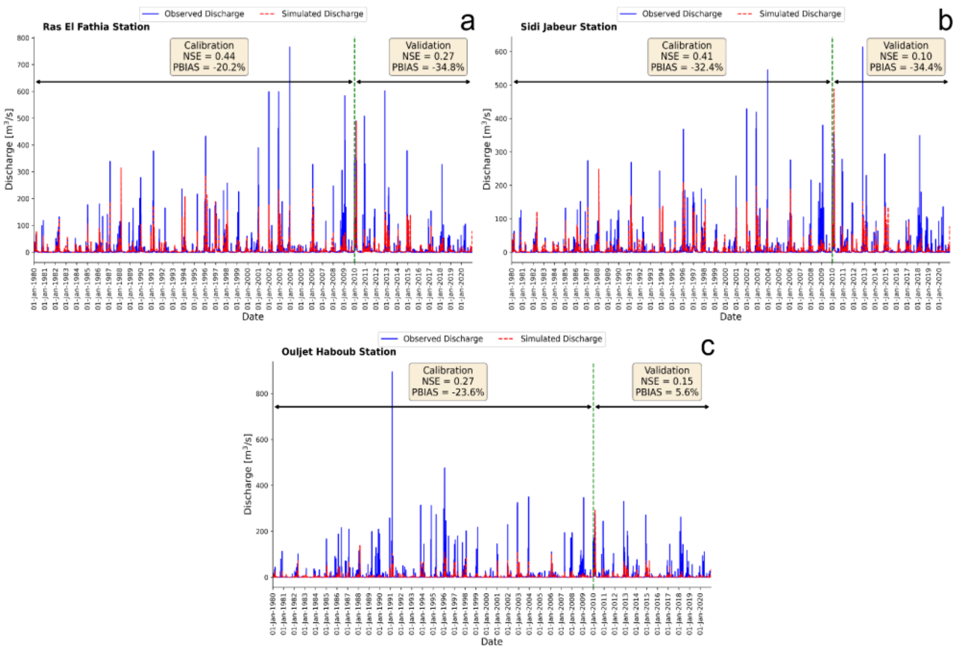

Fig. 5 Observed and simulated daily discharges at (a) RF station, (b) SJ station, and (c) OH station

generation are critical drivers of the watershed's hydrological response. This can be explained by the most impervious substratum of the Grou watershed and its semi-arid climate where high evaporation rates control water availability (Cherrad, 1997) The moderate influence of topographic factors (SLSUBBSN, HRU_SLP) and groundwater delay (GW_DELAY) further indicates that, while surface runoff is dominant, subsurface flow and groundwater recharge play a secondary role in sustaining streamflow. The relatively low sensitivity of channel routing (CH_K2) and baseflow (ALPHA_BF) confirms that streamflow in the Grou watershed is primarily event-driven, with minimal contribution from baseflow, another characteristic feature of semi-arid regions.

Fig. 5 shows the simulated and observed hydrographs during the calibration period (1980-2009) and the validation period (2010-2020) across all stations. A visual comparison indicates that the model had satisfactory performance overall, particularly at the RF and SJ stations. This conclusion is supported by the NSE and PBIAS values presented in the same figures. During the calibration period, the model's performance was satisfactory at the downstream stations RF and SJ, with NSE values of 0.44 and 0.41 respectively, and PBIAS values of -20.2% and -32.4%, respectively. However, the results were suboptimal at the upstream station OH, with a low NSE value of 0.27. The model's performance further declined during validation, with an NSE values of 0.15; however, the relatively low PBIAS values indicate an overall acceptable performance.

3.2 Construction and comparison of the FDCs

One of the essential steps of this study is the construction of the FDCs, therefore, the model's accuracy can be further investigated by comparing observed and simulated plots. Using the HD estimator, FDCs for the selected sites were generated for each year of the 1980-2020 period and compared to the observed FDCs using the NSE coefficient. The results across the stations, presented in Fig. 6 reveal significant variations in predictive accuracy. The SJ and RF stations exhibit higher NSE values, with median values of 0.65 and 0.62, respectively, and minimum values of approximately 0.40, indicating good model performance. These stations also display relatively close NSE values, suggesting that the model's performance remains stable

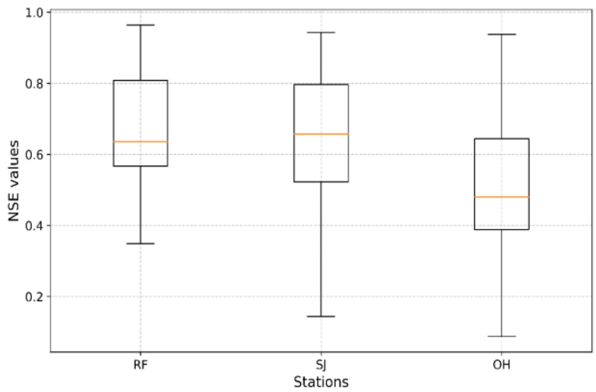

Fig. 6 NSE values of simulated FDCs across all stations

across different years. Conversely, the OH station demonstrates greater variability, with NSE values ranging from 0.1 to nearly 1, and a lower median NSE value of 0.5, reflecting a less reliable model performance. The wider spread of values at OH suggests that the model struggles to capture the full range of flow conditions at this site. While the results at RF and SJ confirm the robustness of the model, the lower performance at OH raises questions regarding the sources of discrepancies, which are further examined in the following section. In particular, the simulated median AFDC, shown in Fig. 7, exhibited NSE values of 0.86, 0.56, and 0.78 at the RF, SJ, and OH stations, respectively, with the main deviations in the plots observed at the high flows.

3.3 Evaluation of data consistency and sources of discrepancies

The overall performance of the model was satisfactory when comparing the simulated and observed daily streamflow, the yearly FDCs and the median AFDCs at RF and SJ, the downstream stations. However, this was not the case for the upstream station OH. Therefore, the double-mass curve method was used to search for possible discrepancies in the streamflow data of the OH and SJ stations. The approach described by Searcy, Hardison and Langbein (1960), plots the cumulative annual runoff of each station against the cumulative annual

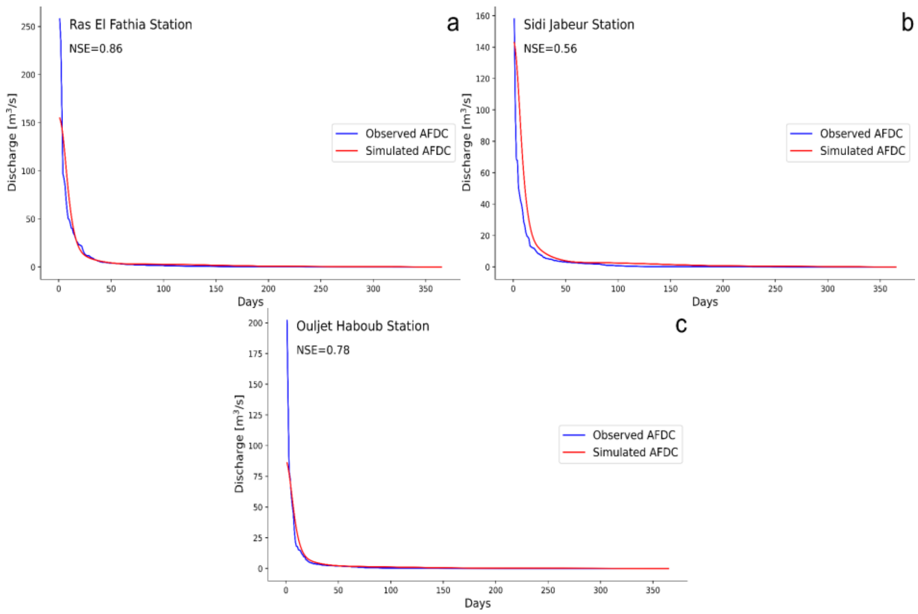

Fig. 7 Observed and simulated median AFDCs at (a) RF station, (b) SJ station, and (c) OH station

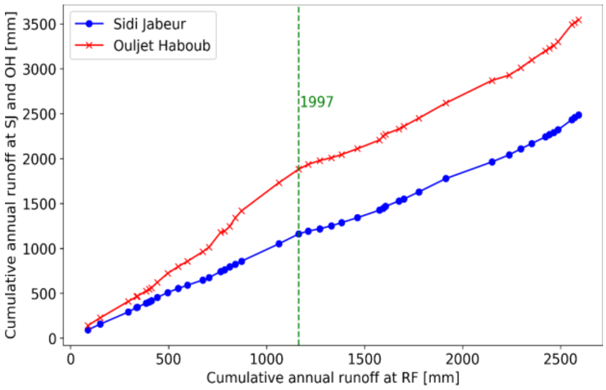

Fig. 8 Double-mass curves of runoff data

Table 6
F-test results for significance of slope breaks in the double-mass curves

Station	F-statistic	Critical value	Results of the test
OH	3.35	2.06	Reject the null hypothesis: Variances are significantly different
SJ	0.069	2.06	Fail to reject the null hypothesis: No significant difference in the variance

runoff of the reference station, which in our case is the RF station since it is the most recent station in the watershed. As shown in Fig. 8, a break in the slope of the plots in 1997 is more prominent for the OH station.

For further investigation, Searcy, Hardison, and Langbein (1960) recommend applying statistical tests to determine if random streamflow variability is the cause behind the slope variation, especially since there were no changes in the data collection method or major physical alterations in the Grou watershed during that specific year. Therefore, the F-test was run to compare the variances of the cumulative runoff before and after 1997 for both the SJ and OH stations against the RF station (Searcy, Hardison, & Langbein, 1960). The results at a 5% significance level are presented in Table 6. They revealed a significant change in the relationship between the runoffs at the OH and RF stations. In contrast, no significant change was detected in the relationship between the runoffs at the SJ and RF stations. Therefore, there is a low probability that the break in the slope is caused by chance or by hydrological conditions; otherwise, it would have been more prominent at the SJ station. The only remaining explanation is a probable error in the OH station data, which could justify the model's poor performance at this station.

The SWAT model successfully captured the event-driven hydrological dynamics of the watershed, as evidenced by the high sensitivity of surface runoff parameters and minimal baseflow influence, which align with the semi-arid, impervious nature of the basin. However, the calibration process, reliant on the NSE statistic, likely overestimated the flashy runoff tendencies, resulting in exaggerated high flows in the simulated FDCs (Lamontagne, Barber, & Vogel, 2020). Additionally, the use of annual FDCs masks seasonal flow variations, which could have tempered the model's surface response. This likely amplified the model's inherent bias toward rapid surface runoff while underrepresenting the moderating influence of sub-seasonal climatic fluctuations. Thus, while the model correctly represented the watershed's dominant processes, the calibration approach inadvertently intensified their extremes.

Despite these inconsistencies, the model's results are overall acceptable. Additionally, this study's approach relies mainly on plotting the FDCs, and as illustrated in Fig. 5, the majority presented NSE values greater than 0.5. Furthermore, the median AFDCs illustrated in Fig.6, used to determine the RoR plants' capacities, showed more than satisfactory accuracy. Consequently, the model can provide reliable estimates of the hydropower potential for the Grou watershed

3.4 Assessment of optimal theoretical hydropower

Following the steps described in section 2.5, the EDCs were plotted for each potential site. The resulting graphs in Fig. 9 exhibit multiple peaks that represent the maximum annual energy. Each maximum value corresponds to the value of optimal theoretical power and optimal discharge. In our case, three local maxima are the most prominent. The first peak is caused by extremely high flows, which last for only a few days. The last peak is caused by low flows that are available for many days of the year. Finally, an intermediate peak offers a compromise between the value of the discharge and its availability. Therefore, three scenarios of hydropower production were considered: high production level, moderate production level, and low production level. The corresponding potential, assuming a 1 m head, is detailed in Fig. 10. The data highlights a significant disparity in power production across different hydropower production scenarios. Under the high

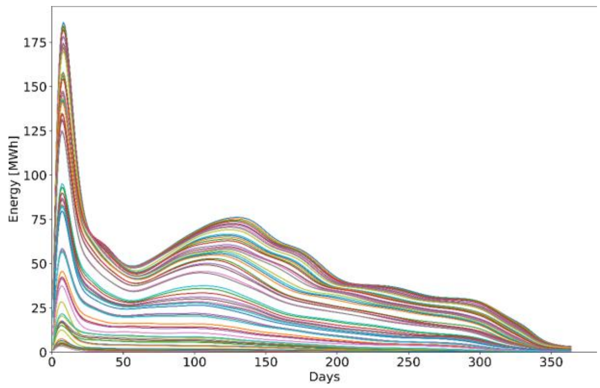

Fig. 9 EDCs at each potential RoR sites

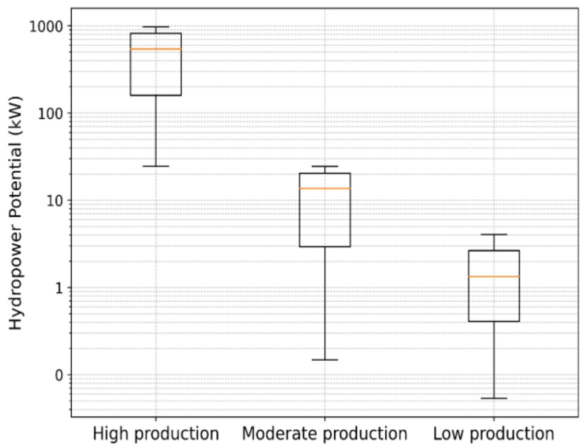

Fig. 10 Hydropower potential of the selected RoR sites across all production levels

Table 7
Hydropower potential, discharge ranges and their availability ranges across all production levels

	Total hydropower (kW)	Days of availability			Discharge in m^3/s		
		Maximum	Average	Minimum	Maximum	Average	Minimum
High production level	31 516	8	7	6	98.9	53.5	2.50
Moderate production level	783.3	140	114	97	2.5	1.3	0.02
Low production level	98.9	298	276	170	0.4	0.2	0.005

production scenario, RoR plants can generate between 24.5 kW and 1000 kW, while the moderate production scenario sees outputs ranging from 0.15 kW to 24.5 kW. The low production scenario, in contrast, yields only 0.05 kW to 4 kW. This variability in power output is a direct consequence of the highly fluctuating flow regime of the Grou watershed. The watershed's largely impervious geological formations result in rapid runoff and high discharges during wet periods, whereas during dry periods, the base flow is significantly reduced (Cherrad, 1997).

The total hydropower potential for each production level is summarized in Table 7. Specifically, the watershed has an estimated potential of 31.5 MW, 783 kW, and 100 kW for the high, moderate, and low production scenarios, respectively. Consequently, in theory, the watershed could generate a total of 32.4 MW per 1 m of head. Such optimal hydropower production could be achieved by using a three-turbine set with different design flows. This setup would allow for the efficient utilization of both low and high discharge periods, ensuring that power generation remains as stable as possible despite seasonal fluctuations.

Regarding the spatial distribution of hydropower potential, as illustrated in Fig. 11, power production increases downstream. The southeastern tributary sites generate more power than the southwestern tributary sites. However, the majority of the watershed's hydropower is produced after the two main tributaries merge. From this confluence to the watershed outlet, an estimated 23.3 MW per 1 m of head is generated, accounting for approximately 72% of the watershed's theoretical hydropower potential. This is primarily due to the assumption of a 1 m head, making the calculated potential highly dependent on increasing discharge downstream. However, as discussed in Section 2.2, the available

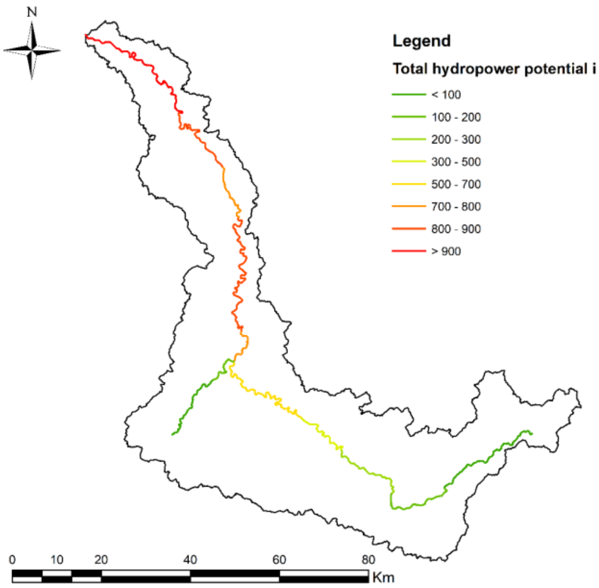

Fig. 11 The total hydropower potential along the rivers of the Grou watershed for a 1 m head

topographical data indicates a minimum altitude difference of 5 m between consecutive projected sites. Consequently, the untapped theoretical potential of the Grou watershed could exceed 32.4 MW, depending on the actual gross head and the elevation of constructed weirs.

The availability of discharge for each production scenario is summarized in Table 7. The hydropower potential of the Grou watershed exhibits significant variability across different production levels. The high production level is highly intermittent, available for an average of 7 days, with peak discharges of 98.9 m^3/s. This suggests that extreme flow conditions are rare and cannot be relied upon for continuous energy production. In contrast, the moderate production level provides a more reliable source, with an average of 114 days, benefiting from steadier discharges around 1.3 m^3/s. The low production level is the most stable, ensuring power generation for up to 298 days per year even at an average discharge of 0.2 m^3/s, making it a valuable baseline energy source.

This pronounced variability in flow conditions highlights the importance of adopting an adaptive turbine configuration capable of harnessing both peak and low-flow periods. While conventional RoR schemes in semi-arid climates typically rely on fixed, low design flows to ensure continuous operation (Tzoraki, 2020), this approach may lead to significant underutilization of the available hydropower potential. By contrast, the modular strategy proposed in this study not only maximizes annual energy capture but also enhances operational flexibility and improves the overall resilience of RoR plants in hydrologically dry contexts such as the Grou basin.

Nevertheless, this strategy also introduces potential trade-offs, as managing several turbines operating under different flow conditions may lead to technical complexity and increased investment costs, particularly for units designed to harness infrequent high flows (Tsuanyo *et al.*, 2023). Furthermore, the selection of discharge levels can have significant ecological implications, as diverting low flows can exacerbate habitat fragmentation and increase stress on aquatic ecosystems, especially during dry periods. Meanwhile, capturing high flows to maximize energy production can substantially alter sediment transport processes and disrupt essential riverine dynamics (Kuriqi *et al.*, 2021).

Despite these challenges, the modular design of RoR systems allows for incremental installation, enabling developers to begin with a small capacity and expand as financial resources or energy demand increase—an approach particularly beneficial in low-income or remote regions. This flexibility, combined with the relatively straightforward licensing procedures typical of RoR projects, enhances the attractiveness of modular schemes (Kuriqi *et al.*, 2021). Furthermore, although climate change projections indicate that RoR hydropower production will be impacted by reduced streamflow, Skoulikaris (2021) highlights that the most significant declines occur during dry months, with less pronounced effects during wet periods. In this context, modular turbines can help offset power losses in low-flow periods by optimizing the capture of higher flows when available.

Table 8
Benchmarking the present study against similar hydropower assessments

Reference	Main objective	Site selection method	Design flow selection	Key assumptions and limitations	Main findings	Innovative aspects
This study	Optimization of RoR hydropower potential in arid climates.	DEM-based approach with equidistant spacing between potential sites.	Design flow derived from hydrological modeling and EDC analysis, using three turbines per site.	No energy losses considered; power generated per meter of head.	Modular turbine configuration can yield up to 32 MW per meter of head in semi-arid watersheds.	Integration of modular turbines per site; EDC-based hydropower optimization in arid climates; Analytical derivation of FDCs from HD estimates; First RoR potential assessment in Morocco using both measured and reanalysis data.
Alcalá *et al.* (2021)	Automated assessment of RoR potential using a GIS-based mesh sweeping approach.	Rectangular mesh-based sweeping, using topographic and hydraulic parameters.	Monthly modeled streamflow.	Constraints on headrace canal and penstock lengths; no plant interference or head losses considered.	The optimal configuration—1500 m headrace and 2000 m penstock—was identified, highlighting the often-overlooked influence of headrace length on system optimization.	Raster-based mapping for RoR potential that enables optimization of site selection and component sizing.
Dhaubanjar *et al.* (2024)	Evaluation of sustainable RoR potential in the Upper Indus Basin under various constraints.	DEM-based approach with equidistant spacing between potential sites.	Annual average discharge for theoretical potential calculations; Q_{30}, Q_{40}, and Q_{80} flows for technical potential calculations.	Technical and economic limitations, along with water use, land use, and geo-hazard considerations.	Only 2 - 10% of the theoretical potential is sustainable, with substantial untapped hydropower in two sub-basins.	Development of a comprehensive multi-scale framework for evaluating sustainable RoR hydropower potential.
Moshe & Tegegne (2022)	Assessment of RoR hydropower feasibility in data-scarce basins using GIS and SWAT modeling.	DEM-based approach with equidistant spacing between potential sites.	Q_{50}, Q_{75}, and Q_{90} flows selected from period of record FDC.	Transfer FDCs from gauged to the ungauged watershed. Constraints on available head and stream order. No energy losses considered	A total of 103 RoR sites identified, with a combined potential exceeding 33.03 MW in a data-scarce basin.	Application of GIS-based multi-criteria decision-making for prioritizing RoR sites in data-scarce regions.
Magaju, Cattapan, & Franca, (2020)	Identification of optimal RoR hydropower locations and capacities in data-scarce regions using global datasets.	Optimization model targeting minimum specific cost for RoR plant development.	Q_{40} flow selected from analytically derived FDC	A maximum capacity of 100 MW; conveyance lengths limits; minimum environmental flow.	A total of 79 RoR projects identified, with a combined capacity of 320 MW.	An open-source model for cost-optimized RoR development using analytical FDC derivation from global datasets.
Ndhlovu & Woyessa (2022)	Evaluating small hydropower potential in ungauged watersheds under projected climate change.	GIS and DEM-based selection with criteria including head, distance between weir and turbine, and stream cross-section.	Q_{80} flow selected from period of record FDC and projected FDC under climate. change scenarios	Transfer calibrated parameters from gauged to the ungauged watershed.	Six viable sites were identified; a 5-10% increase in RoR potential is projected under RCP 8.5.	Novel integration of SWAT modeling, RCP-based climate projections, GIS analysis, and regional FDCs to inform RoR design in ungauged basins.

In the Moroccan context, challenges remain regarding the share of renewable energy in total final consumption (7.9 %). Similarly, the country's CO_2 emissions from fuel combustion per total electricity output remain moderate yet must be further reduced to meet climate goals. (Sachs, Lafortune, & Fuller 2024). By optimizing RoR hydropower schemes and proposing a framework adapted to dry climates, this study provides a pathway to increase the share of low-carbon energy production and strengthen resilience against future hydrological uncertainties. As such, it directly supports Morocco's efforts to improve its Sustainable Development Goals 7 (Affordable and Clean Energy) and 13 (Climate Action) indicators and reduce its dependence on fossil fuels.

To clearly position the contribution of this study within the broader body of research, Table 8 presents a comparative synthesis of some recent works on RoR hydropower assessment. In comparison with the existing literature, the present study distinguishes itself by introducing a novel approach estimating turbine design flow, specifically developed to maximize hydropower. It also integrates modular turbine assessment under arid climatic conditions and proposes a practical framework for evaluating RoR potential in dry watersheds, applied for the first time in the Moroccan context, where such projects remain largely unexplored. These contributions offer new insights into the optimization of RoR systems under future hydrological uncertainties.

Consequently, our study findings are encouraging and offer both communities and authorities promising perspectives of green power production through the implementation of RoR plants. These facilities offer a reliable alternative to storage plant projects to achieve the goals set for hydropower production in Morocco, since the large-scale hydropower plants often face financial, regulatory, and social challenges (IRENA, 2023b). Therefore, we recommend that water resource managers integrate modular turbine technology into RoR projects with small hydraulic heads of less than 10 meters, depending on available funds and the topography of the locations. Furthermore, these calculations can be further improved by considering the projects' technical limitations and economic feasibility. Factors such as head losses across various plant components and turbine efficiency significantly affect energy output. Additionally, all combined plant implementation costs should be accounted for when identifying potential sites.

4. Conclusion

While hydropower is a reliable and sustainable energy source, its viability in arid regions is constrained by high evaporation and low precipitation. In such environments, RoR systems offer a practical alternative, yet their efficiency is inherently linked to seasonal and hydrological variability. Therefore, this study presents an exhaustive approach to assessing the hydropower potentialities of a semi-arid basin. It aims to optimize hydropower production for RoR plants through the usage of modular turbines to capture a wide range of discharges. The approach integrates hydrological modeling using the SWAT model to estimate river discharge, followed by the development of FDCs and EDCs to identify optimal design flows for modular turbines. This methodology was applied to the Grou watershed in Morocco, a tributary of the Bouregreg basin, where hydropower potential remains largely unexploited.

This study establishes that the Grou watershed possesses a theoretical RoR hydropower potential of 32.4 MW per meter of head across 60 potential sites, namely 31 516 kW/m during high flow periods, 783.3 kW/m during moderate flow periods, and 98.9 kW/m during low flow periods. This potential was identified through the EDC analysis, which reveals multiple optimal discharge choices and demonstrates that modular turbines can maximize energy extraction for nearly ten months of the year by operating across different flow regimes. Furthermore, considering the existing topography and potential weir heights, the available head could be increased by at least 5 m, therefore, the actual hydropower potential significantly exceeds the theoretical estimates.

These findings confirm that RoR schemes can remain resilient in semi-arid climates and under climate-change scenarios when supported by a tailored framework that integrates modular turbine configurations. Although this study focuses on theoretical hydropower estimation, it nevertheless offers a foundation for preliminary site selection. Final feasibility assessments should include technical, economic, and environmental evaluations to determine the viability of specific projects.

In conclusion, this research provides a methodological framework for evaluating and optimizing RoR hydropower in semi-arid watersheds. By leveraging modular turbine technology, these plants can adapt to seasonal discharge fluctuations and extend power generation periods, offering an efficient and sustainable energy solution.

Nomenclature

Abbreviation	Description
AFDC	Annual flow-duration curve
BIM	Building Information Modeling
DEM	Digital elevation model
EDC	Energy-duration curve
FDC	Flow-duration curve
GIS	Geographic information system
HD	Harrell-Davis
LULC	Land Use/Land cover
OH	Ouljet Haboub station
PDC	Power-duration curve
RF	Ras El Fathia station
RoR	Run-of-river
RS	Remote sensing
SJ	Sidi Jabeur station
SWAT	Soil and Water Assessment Tool

Notations	Description
d	Number of days of power availability in the run-of-river plant
E	Energy produced by a run-of-river plant [Wh]
H	Hydraulic head [m]
$I_x[a,b]$	Incomplete beta function
NSE	Nash-Sutcliffe coefficient
n	Number of daily streamflow observations in a year
P	Power produced by a run-of-river plant [W]
PBIAS	Percent bias [%]
p	Probability of exceedance [%]
Q	River discharge [m^3/s]
$Q_{p,HD}$	HD estimate of the pth quantile with a p% probability of exceedance [m^3/s]
Q_p	Discharge with a p% probability of exceedance [m^3/s]
q_i	Daily streamflow observation [m^3/s]
W_i	Harrell-Davis estimator weights
ɣ	Specific weight of water [N/m3]

Author Contributions: I.E.K and M.D.H: Conceptualization, material preparation, data collection, analysis, writing—original draft, A.B., A.A and D.K; review, editing and validation. All authors have read and agreed to the published version of the manuscript.

Funding: The authors received no financial support for the research, authorship, and/or publication of this article.

Conflicts of Interest: The authors declare no conflict of interest.

References

Alcalá, G., Grisales-Noreña, L.F., Hernandez-Escobedo, Q., Muñoz-Criollo, J.J., & Revuelta-Acosta, J.D. (2021). SHP assessment for a run-of-river (RoR) scheme using a rectangular mesh sweeping approach (MSA) based on GIS. *Energies*, 14(11), 3095. https://doi.org/10.3390/en14113095

Alduchov, O.A., & Eskridge, R.E. (1996). Improved Magnus form approximation of saturation vapor pressure. *Journal of Applied Meteorology*, 35(4), 601–609. https://doi.org/10.1175/1520-0450(1996)035<0601:IMFAOS>2.0.CO;2

Amougou, C. B., Tsuanyo, D., Fioriti, D., Kenfack, J., Aziz, A., & Abiama, P. E. (2022). LCOE-Based Optimization for the Design of Small Run-of-River Hydropower Plants. *Energies*, 15(20), 7507. https://doi.org/10.3390/en15207507

Arnold, J.G., Moriasi, D. N., Gassman, P. W., Abbaspour, K. C., White, M. J., Srinivasan, R., Santhi, C., Harmel, R. D., van Griensven, A., Van Liew, M. W., Kannan, N., & Jha, M. K. (2012). SWAT: Model use, calibration, and validation. *Transactions of the ASABE*, 55(4), 1491–1508. https://doi.org/10.13031/2013.42256

Arnold, J.G., Srinivasan, R., Muttiah, R.S., & Williams, J.R. (1998). Large area hydrologic modeling and assessment Part 1, model development. *Journal of the American Water Resources Association*, 34(1), 73-89.

Bejarano, M. D., Sordo-Ward, A., Gabriel-Martin, I., & Garrote, L. (2019). Tradeoff between economic and environmental costs and benefits of hydropower production at run-of-river-diversion schemes under different environmental flows scenarios. *Journal of Hydrology*, 572, 790–804. https://doi.org/10.1016/J.JHYDROL.2019.03.048

Bhattarai, R., Mishra, B. K., Bhattarai, D., Khatiwada, D., Kumar, P. & Meraj, G. (2024). Assessing Hydropower Potential in Nepal's Sunkoshi River Basin: An Integrated GIS and SWAT Hydrological Modeling Approach. *Scientifica*, 2024. https://doi.org/10.1155/2024/1007081

Blum, A.G., Archfield, S.A., & Vogel, R.M. (2017). On the probability distribution of daily streamflow in the United States. *Hydrology and Earth System Sciences*, 21(6), 3093–3103. https://doi.org/10.5194/hess-21-3093-2017

CARD, ISU. (2023). *SWAT literature database for peer-reviewed journal articles*. https://www.card.iastate.edu/swat_articles/. Accessed on 15 Mai 2025

Cherrad, B. (1997). *Le bassin versant de l'oued Grou (plateau central marocain): étude hydro-climatologique*. PhD thesis. Paul Verlaine University.

Dhaubanjar, S., Lutz, A. F., Pradhananga, S., Smolenaars, W., Khanal, S., Biemans, H., Nepal, S., Ludwig, F., Shrestha, A. B., & Immerzeel, W. W. (2024). From theoretical to sustainable potential for run-of-river hydropower development in the upper Indus basin. *Applied Energy*, 357, 122372. https://doi.org/10.1016/j.apenergy.2023.122372

Dilnesa, W. (2022). GIS and hydrological model-based hydropower potential assessments of Temcha watershed. *International Journal of Environment and Geoinformatics*, 9(1), 97-101. https://doi.org/10.30897/ijegeo.783157

El Hafdaoui, H., Khallaayoun, A & Al-Majeed, S. (2025). Renewable Energies in Morocco: A comprehensive review and analysis of current status, policy framework, and prospective potential. *Energy Conversion and Management X*. 26, 100967. https://doi.org/10.1016/j.ecmx.2025.100967

ESMAP (2021) *Assessing and Mapping Renewable Energy Resources*, 2nd edn. World Bank, Washington, DC.

ESRI. (2013). *World Countries Generalized*. https://hub.arcgis.com/maps/esri::world-countries-generalized Accessed on 2 September 2024.

FAO. (1971-1981). *FAO-UNESCO Soil Map of the World*. https://data.apps.fao.org/map/catalog/srv/eng/catalog.search#/metadata/446ed430-8383-11db-b9b2-000d939bc5d8

Garcia, X., Estrada, L., Llorente, O., & Acuña, V. (2024). Assessing small hydropower viability in water-scarce regions: environmental flow and climate change impacts using a SWAT+ based tool. *Environmental Sciences Europe*, 36, 126. https://doi.org/10.1186/s12302-024-00938-1

Golgojan, A.D., White, C.J. & Bertram, D. (2025). An assessment of run of river hydropower potential in Great Britain. *Proceedings of the Institution of Civil Engineers - Water Management,* 178(1), 42-61. https://doi.org/10.1680/jwama.23.00056

Harrell, F.E., & Davis, C.E. (1982). A new distribution-free quantile estimator. *Biometrika*, 69(3), 635–640. https://doi.org/10.2307/2335999

Hedger, R.D., Kenawi M.S., Sundt-Hansen, L.E., Bakken, T.H., & Sandercock, B.K. (2025). Evaluating environmental impacts of micro, mini and small hydropower plants in Norway. *Journal of Environmental Management*, 373, 123521. https://doi.org/10.1016/j.jenvman.2024.123521

Ibrahim, M., Imam, Y., & Ghanem, A. (2019). Optimal planning and design of run-of-river hydroelectric power projects. *Renewable Energy*, 141, 858-873. https://doi.org/10.1016/j.renene.2019.04.009

IEA. (2021). Hydropower special market report. IEA, Paris.

IRENA. (2023a), Renewable energy benefits: Leveraging local capacity for small-scale hydropower, IRENA, Abu Dhabi.

IRENA. (2023b). The changing role of hydropower: Challenges and opportunities. IRENA, Abu Dhabi.

IRENA. (2024). *Renewable energy statistics 2024*. IRENA, Abu Dhabi.

Janjić, J., & Tadić, L. (2023). Fields of application of SWAT hydrological model—A review. *Earth*, 4(2), 331-344. https://doi.org/10.3390/earth4020018

JAXA. (2014). ALOS PALSAR Digital Elevation Model. https://doi.org/10.5067/Z97HFCNKR6VA Accessed on 24 October 2023

Kalin, L., Isik, S., Schoonover, J.E., & Lockaby, B.G. (2010). Predicting water quality in unmonitored watersheds using artificial neural networks. *Journal of Environmental Quality*, 39(4), 1429–1440. https://doi.org/10.2134/jeq2009.0441

Kamran, M. (2022). *Energy sources and technologies*. In: *Fundamentals of Smart Grid Systems*. 1st edn. Academic Press, Amsterdam. Chapter 2, pp. 23-69. https://doi.org/10.1016/B978-0-323-99560-3.00010-7

Karra, K., Kontgis, C., Statman-Weil, Z., Mazzariello, J.C., Mathis, M.M., & Brumby, S.P. (2021). Global land use/land cover with Sentinel 2 and deep learning. *2021 IEEE International Geoscience and Remote Sensing Symposium IGARSS*, 4704-4707. https://doi.org/10.1109/IGARSS47720.2021.9553499

Killingtveit, Å. (2020). *Hydroelectric Power*. In: Letcher, T. M. (ed.), *Future Energy: Improved, Sustainable and Clean Options for Our Planet*. 3rd edn. Elsevier, Amsterdam. Chapter 15, pp. 315–330. https://doi.org/10.1016/B978-0-08-102886-5.00015-3

Kuriqi, A., Pinheiro, A., Sordo-Ward, A., Bejarano, M. & Garrote, L. (2021). Ecological impacts of run-of-river hydropower plants—Current status and future prospects on the brink of energy transition. *Renewable and Sustainable Energy Reviews*, 142. https://doi.org/10.1016/j.rser.2021.110833

Lamontagne, J. R., Barber, C. A., & Vogel, R. M. (2020). Improved Estimators of Model Performance Efficiency for Skewed Hydrologic Data. *Water Resources Research*, 56(9). https://doi.org/10.1029/2020WR027101

Leong, C., & Yokoo, Y. (2021). A step toward global-scale applicability and transferability of flow duration curve studies: A flow duration curve review (2000–2020). *Journal of Hydrology*, 603, 126984. https://doi.org/10.1016/j.jhydrol.2021.126984

Magaju, D., Cattapan, A., & Franca, M. (2020). Identification of run-of-river hydropower investments in data scarce regions using global data. *Energy for Sustainable Development*, 58, 30-41. https://doi.org/10.1016/j.esd.2020.07.001

Malhan, P., & Mittal, M. (2021). Evaluation of different statistical techniques for developing cost correlations of micro hydropower plants. *Sustainable Energy Technologies and Assessments*, 43, 100904. https://doi.org/10.1016/j.seta.2020.100904

Moriasi, D.N., Arnold, J.G., Van Liew, M.W., Bingner, R.L., Harmel, R.D., & Veith, T.L. (2007). Model evaluation guidelines for systematic quantification of accuracy in watershed simulations. *Transactions of the ASABE*, 50, 885-900. https://doi.org/10.13031/2013.23153

Moshe, A., & Tegegne, G. (2022). Assessment of run-of-river hydropower potential in the data-scarce region, Omo-Gibe Basin, Ethiopia. *International Journal of Energy and Water Resources,* 6, 531–542. https://doi.org/10.1007/s42108-022-00192-2

Muñoz Sabater, J. (2019). *ERA5-Land hourly data from 1950 to present.* Copernicus Climate Change Service (C3S), Climate Data Store (CDS). https://doi.org/10.24381/cds.e2161bac . Accessed on 15 October 2023.

Nash, J.E., & Sutcliffe, J.V. (1970). River flow forecasting through conceptual model. part 1—A discussion of principles. *Journal of Hydrology*, 10(3), 282-290. https://doi.org/10.1016/0022-1694(70)90255-6

Natural Earth. (2009). *Cross blended hypso with relief, water, drains, and ocean bottom.* https://www.naturalearthdata.com/downloads/10m-cross-blend-hypso/cross-blended-hypso-with-relief-water-drains-and-ocean-bottom/ . Accessed on 2 September 2024

Nedaei, M., & Walsh, P.R. (2022). Technical performance evaluation and optimization of a run-of-river hydropower facility. *Renewable Energy*, 182, 343-362. https://doi.org/10.1016/j.renene.2021.10.021

Ndhlovu, G.Z., & Woyessa, Y.E. (2022). Streamflow Analysis in Data-Scarce Kabompo River Basin, Southern Africa, for the Potential of Small Hydropower Projects under Changing Climate. *Hydrology*, 9(8). https://doi.org/10.3390/hydrology9080149

Pranoto, B., Hartulistiyoso, E., Aidi, M.N., Sutrisno, D., Nahib, I., Purwono, N., Hudayat, N., Rais, A.F., & Rahmila, Y.I. (2024). Assessing the sustainability of small hydropower sites in the Citarum Watershed, Indonesia employing CA-Markov and SWAT models. *Water Supply*, 24(9), 3253–3268. https://doi.org/10.2166/ws.2024.209

Sarigil, G., Cavus, Y., Aksoy, H. & Eris, E. (2024). Frequency curves of high and low flows in intermittent river basins for hydrological analysis and hydraulic design. *Stochastic Environmental Research and Risk Assessment,* 38, 3079–3092. https://doi.org/10.1007/s00477-024-02732-0

Searcy, J.K. (1959). *Flow duration curves. Manual of Hydrology: Part 2. Low-Flow Techniques. U.S.* Government Printing Office, Washington, D.C.

Searcy, J.K., Hardison, C.H., & Langbein, W.B. (1960). *Double mass curves. Manual of Hydrology: Part 1. General Surface Water Techniques.* U.S. Government Printing Office, Washington, D.C.

Shrestha, J.P., Pahlow, M., & Cochrane, T.A. (2020). Development of a SWAT hydropower operation routine and its application to assessing hydrological alterations in the Mekong. *Water*, 12(8), 2193. https://doi.org/10.3390/w12082193

Skoulikaris, C. (2021). Run-Of-River Small Hydropower Plants as Hydro-Resilience Assets against Climate Change. *Sustainability,* 13(4), 14001. https://doi.org/10.3390/su132414001

SWAT (Version 2012.10.5.24) (2012). Texas A&M University, Texas A&M AgriLife Research, USDA. Available at: https://swat.tamu.edu/software/arcswat/

SWAT-CUP (Version 2019). (2007). Water Weather Energy Ecosystem. Available at: https://www.2w2e.com/home/SwatCup

Tan, M. L., Gassman, P. W., Yang, X., & Haywood, J. (2020). A review of SWAT applications, performance and future needs for simulation of hydro-climatic extremes. *Advances in Water Resources*, 143, 103662. https://doi.org/10.1016/j.advwatres.2020.103662

Thakur, C., Teutschbein, C., Kasiviswanathan, K. S., & Soundharajan, B.-S. (2024). Mitigating El Niño impacts on hydro-energy vulnerability through identifying resilient run-of-river small hydropower sites. *Journal of Hydrology: Regional Studies*, 51, 101622. https://doi.org/10.1016/j.ejrh.2023.101622

Tsuanyo, D., Amougou, B., Aziz, A., Nnomo, B., Fioriti, D., & Kenfack, J. (2023). Design models for small run-of-river hydropower plants: a review. *Sustainable Energy Research*, 10(3). https://doi.org/10.1186/s40807-023-00072-1

Tzoraki, O. (2020). Operating small hydropower plants in Greece under intermittent flow uncertainty: The case of Tsiknias River (Lesvos). Challenges, 11(2),17. https://doi.org/10.3390/challe11020017

UNIDO & ICSHP (2022) *World Small Hydropower Development Report 2022.* United Nations Industrial Development Organization, Vienna, Austria; International Center on Small Hydro Power, Hangzhou, China

Védie, H-L. (2020). *Renewable energy in Morocco: A reign-long project.* https://www.policycenter.ma/publications/renewable-energy-morocco-reign-long-project . Accessed on 23 July 2024.

Vogel, R.M., & Fennessey, N.M. (1994). Flow duration curves I: New interpretation and confidence intervals. *Journal of Water Resources Planning and Managemen*t, 120(4), 485-504. https://doi.org/10.1061/(ASCE)0733

Wangchuk, J., Banihashemi, S., Abbasianjahromi, H. & Antwi-Afari, M.F. (2024). Building Information Modelling in Hydropower Infrastructures: Design, Engineering and Management Perspectives. *Infrastructures*, 9(7), 98. https://doi.org/10.3390/infrastructures9070098